Journal of Materials Chemistry C

PAPER

View Article Online
View Journal | View Issue

Cite this: J. Mater. Chem. C, 2016, 4, 5981

Air-stable n-channel organic field-effect transistors based on charge-transfer complexes including dimethoxybenzothienobenzothiophene and tetracyanoquinodimethane derivatives†

Toshiki Higashino,‡*[a] Masaki Dogishi,§[a] Tomofumi Kadoya,¶[a] Ryonosuke Sato,[a] Tadashi Kawamoto[a] and Takehiko Mori*[ab]

Received 15th April 2016,
Accepted 29th May 2016

DOI: 10.1039/c6tc01532h

www.rsc.org/MaterialsC

A new donor molecule 3,8-dimethoxy-[1]benzothieno[3,2-*b*][1]benzothiophene (DMeO-BTBT) is synthesized and the charge-transfer complexes with fluorinated 7,7,8,8-tetracyanoquinodimethane (F_n-TCNQ; n = 0, 2, and 4) are prepared. All complexes (DMeO-BTBT)(F_n-TCNQ) have mixed stack structures, and the thin-film and single-crystal organic transistors show n-channel transistor performance both in vacuum and in air even after one-year storage. Although the performance and stability of the thin-film transistors are improved according to the acceptor ability of F_n-TCNQ, all single-crystal transistors exhibit similar performance and excellent air stability, among which the (DMeO-BTBT)(F_2-TCNQ) transistor exhibits the highest mobility of 0.097 $cm^2\ V^{-1}\ s^{-1}$.

Introduction

Organic field-effect transistors (OFETs) have attracted considerable attention as an important component of flexible electronics.[1–4] Among various organic semiconductors, [1]benzothieno[3,2-*b*][1]-benzothiophene (BTBT) derivatives are known to show high field-effect mobility and excellent stability.[5,6] A strong tendency to form a highly ordered herringbone packing is characteristic of the BTBT derivatives.[7] In particular, C8-BTBT with octyl groups shows improved solubility in organic solvents and very high mobility even in solution-processed devices.[8]

Recently, organic charge-transfer (CT) complexes incorporating BTBT derivatives have been reported.[9–11] The complex of the unsubstituted BTBT with an octahedral anion, $(BTBT)_2PF_6$, shows as high conductivity as 1500 S cm^{-1} at room temperature, though this complex undergoes a metal–insulator transition at low temperatures.[10] This complex consists of BTBT columns arranged orthogonally in a windmill manner, so the electronic structure is highly one-dimensional. Alkyl substituted BTBT derivatives (C*n*BTBT) form CT complexes with 7,7,8,8-tetracyanoquinodimethane (TCNQ) and fluoro TCNQ (F_n-TCNQ).[11] Although these CT complexes have mixed stacks, the thin-film transistors show the electron mobility of the 10^{-2} $cm^2\ V^{-1}\ s^{-1}$ order, and the single-crystal transistor achieves at most 0.4 $cm^2\ V^{-1}\ s^{-1}$. Ambipolar transport has been also observed in the single-crystal transistor of the TCNQ complex.[11a,12] Since mix-stacked CT complexes are composed of donor and accepter molecules, the transistors potentially exhibit p-channel, n-channel, and even ambipolar properties depending on the energy levels.[13] However, many CT complexes including TCNQ show only n-channel transistor properties.[11,14] Owing to the strong electron acceptor ability, single-component TCNQ shows air-stable n-channel transistor properties in the thin films and the crystals.[15,16] Although the single-crystal transistors of TCNQ show high performance, the thin-film transistors are not easily obtained due to the high vapor pressure.[15] Because air-stable n-channel transistor materials are still limited,[17] it is interesting to investigate CT complexes as air-stable n-channel organic transistor materials.

In this work, we have investigated TCNQ complexes of BTBT with methoxy groups, 3,8-dimethoxy-BTBT (DMeO-BTBT, Scheme 1). BTBT has the highest occupied molecular orbital (HOMO) level at

[a] Department of Organic and Polymeric Materials, Tokyo Institute of Technology, O-okayama, Meguro-ku, Tokyo 152-8552, Japan.
E-mail: thigashino@issp.u-tokyo.ac.jp, mori.t.ae@m.titech.ac.jp
[b] ACT-C, JST, Honcho, Kawaguchi, Saitama 332-0012, Japan

† Electronic supplementary information (ESI) available: CCDC contain the supplementary crystallographic information for DMeO-BTBT and its CT complexes. Additional information for synthesis, optical and electrochemical properties, crystal structures, band calculations, degree of charge transfer, device fabrication, and thin-film transistor characteristics in vacuum and in air together with those after one-year storage. CCDC 1409469–1409472. For ESI and crystallographic data in CIF or other electronic format see DOI: 10.1039/c6tc01532h

‡ Present address: The Institute for Solid State Physics, The University of Tokyo, Kashiwa, Chiba 277-8581, Japan.
§ Present address: Imaging Science and Engineering Laboratory, Tokyo Institute of Technology, Yokohama, Kanagawa 226-8503, Japan.
¶ Present address: Graduate School of Material Science, University of Hyogo, Kamigori, Hyogo 678-1205, Japan.

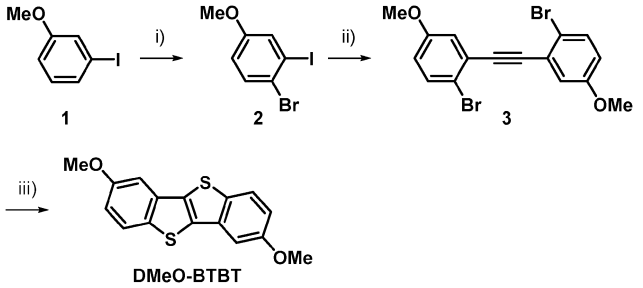

Scheme 1 Synthesis of DMeO-BTBT: (i) NBS/DMF, 80 °C, 4 h, 99%; (ii) $PdCl_2(PPh_3)_2$, CuI, DBU, H_2O, TMS–acetylene/toluene, 60 °C, 18 h, 65%; (iii) CuI, $Na_2S{\cdot}9H_2O$, I_2/NMP, 120 °C, 48 h, 21%.

a very deep position (−5.65 eV).[10a] Accordingly, we have attempted to improve the donor ability by introducing electron donating substituents. DMeO-BTBT is combined with TCNQ derivatives, and three CT complexes, (DMeO-BTBT)(TCNQ), (DMeO-BTBT)(2,5-F_2-TCNQ), and (DMeO-BTBT)(F_4-TCNQ) are obtained. We have investigated the thin-film and single-crystal transistor properties.

Experimental

The synthesis of DMeO-BTBT is outlined in Scheme 1. Bromination of 3-iodoanisole (**1**) with *N*-bromosuccinimide (NBS) in *N*,*N*-dimethylformamide (DMF) gave 4-bromo-3-iodoanisole (**2**).[18] Modified Sonogashira coupling of **2** with a palladium catalyst afforded 1,2-bis(2-bromo-5-methoxyphenyl)acetylene (**3**).[19] Subsequently, heating a *N*-methylpyrrolidine (NMP) solution of **3** with sodium sulfide in the presence of a copper catalyst and excess iodine resulted in the ring formation to afford 3,8-dimethoxy-BTBT (DMeO-BTBT).[5] Charge-transfer complexes of DMeO-BTBT with F_n-TCNQ (n = 0, 2, 4) were grown by mixing the acetonitrile solutions.

Thin films of CT complexes (DMeO-BTBT)(F_n-TCNQ) were deposited by vacuum evaporation of the complexes on a tetratetracontane (TTC)-modified SiO_2/Si substrate, where TTC was used as a passivation layer.[20] The top-contact source and drain electrodes were fabricated by evaporating (TTF)(TCNQ) through a shadow mask with the channel length of 100 μm and the width of 1 mm.[21–23] For single-crystal transistors, crystals of CT complexes were grown by the recrystallization in acetonitrile. The single-crystal transistors were fabricated by using polystyrene (PS) as a passivation layer and carbon paste as source-drain electrodes.[24] The channel direction was determined by the single-crystal X-ray diffraction to be parallel to the crystal long axis corresponding to the molecular stacking (crystallographic *c*) axis. The transistor characteristics were measured under vacuum (10^{-4} Pa) and in an ambient atmosphere. The mobility was evaluated in the saturated region.

Results and discussion

Electrochemical properties and crystal structure of DMeO-BTBT

The electrochemical properties were studied by cyclic voltammetry. DMeO-BTBT shows one irreversible oxidation wave,

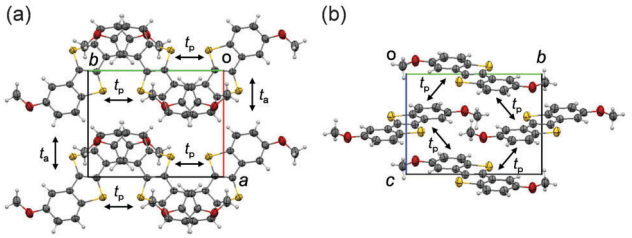

Fig. 1 Crystal structure of DMeO-BTBT viewed along (a) the *c* axis, and (b) the *a* axis. Transfer integrals: t_p = −14.2, t_a = −17.0 meV.

from which the HOMO energy level is estimated to be located at −5.57 eV below the vacuum level. DMeO-BTBT is a slightly stronger donor than the unsubstituted BTBT (−5.65 eV),[10a] because the methoxy groups act as electron-donating groups similarly to alkyl groups; the HOMO level of 2,7-dialkyl-BTBT is located at *ca.* −5.5 eV.[7a]

Single-crystals of DMeO-BTBT for the X-ray structure analysis were grown by recrystallization from the ethyl acetate solution. The molecular packing is depicted in Fig. 1. The crystal belongs to a monoclinic system with the space group $P2_1/c$. The half molecule is crystallographically independent. Unlike the herringbone structure universally observed in BTBT derivatives, the DMeO-BTBT molecules form brickwork-like stacks similar to dimethyldicyanoquinonediimine (DMDCNQI).[25] Along the *c*-axis, two different layers parallel to the DMeO-BTBT planes are alternately stacked with the approximate interplanar spacing of 3.53 Å. One layer consists of parallel molecules, but the molecular long axis of another layer is tilted by 70°.

Crystal structures of the CT complexes

Electrochemical crystallization of DMeO-BTBT cation-radical salts with inorganic anions was attempted expecting the slightly longer DMeO-BTBT molecules alter the orthogonal molecular packing of $(BTBT)_2PF_6$, but the crystals were not obtained. Needle-like black crystals of the TCNQ complexes with the typical dimensions as large as 40 × 1 × 1 mm^3 were obtained by diffusion method from the acetonitrile solutions.

Single crystal X-ray structure analyses were carried out for (DMeO-BTBT)(TCNQ), (DMeO-BTBT)(F_2-TCNQ) and (DMeO-BTBT)(F_4-TCNQ). Table 1 lists the crystallographic data. The molecular arrangements and the intermolecular interactions are depicted in Fig. 2. All crystals belong to a triclinic system with the space group $P\bar{1}$. Respective half donor and acceptor molecules are crystallographically independent; each molecule is located on an inversion center. The unit cell contains one donor and one acceptor molecules, so that the donor/acceptor ratio is 1 : 1. All complexes consist of mixed stacks, where the interplanar distances between the donor and acceptor planes are approximately 3.38, 3.38, and 3.36 Å, respectively; all interplanar distances are equivalent owing to the inversion center at the molecular center. In the (DMeO-BTBT)(F_2-TCNQ), the fluorine atoms have positional disorder with occupancy 84% for the majority position and 16% for the minority position (Fig. S3, ESI†). The nonequivalent occupancy is related to the steric hindrance of the sulfur atoms.

Table 1 Crystallographic data of DMeO-BTBT and (DMeO-BTBT)(F_n-TCNQ) (n = 0, 2, and 4)

	DMeO-BTBT	(DMeO-BTBT)(TCNQ)	(DMeO-BTBT)(F_2-TCNQ)	(DMeO-BTBT)(F_4-TCNQ)
Formula	$C_{16}H_{12}O_2S_2$	$C_{28}H_{16}N_4O_2S_2$	$C_{28}H_{14}F_2N_4O_2S_2$	$C_{28}H_{12}F_4N_4O_2S_2$
Formula weight	300.39	504.58	540.56	576.54
Crystal system	Monoclinic	Triclinic	Triclinic	Triclinic
Space group	$P2_1/c$	$P\bar{1}$	$P\bar{1}$	$P\bar{1}$
Z	2	1	1	1
a (Å)	8.286(3)	8.693(3)	7.777(2)	7.971(3)
b (Å)	10.555(4)	9.371(4)	11.695(4)	11.720(6)
c (Å)	7.814(4)	7.302(4)	7.117(3)	7.066(3)
α (°)	90	93.55(4)	94.34(3)	94.55(4)
β (°)	95.42(3)	97.81(4)	105.31(3)	105.54(3)
γ (°)	90	89.44(3)	72.63(2)	71.28(3)
V (Å^3)	680.3(4)	588.2(5)	595.8(4)	602.4(5)
ρ (g cm^{-3})	1.466	1.424	1.506	1.589
Total reflns.	2339	4063	4123	4170
Unique reflns. (R_{int})	1985 (0.0191)	3417 (0.0215)	3462 (0.0285)	3503 (0.0598)
R_1	0.0327	0.0396	0.0568	0.0964
wR_2	0.0947	0.1055	0.1597	0.3494
GOF	1.018	1.030	0.955	1.311
Temperature (K)	298	298	298	298

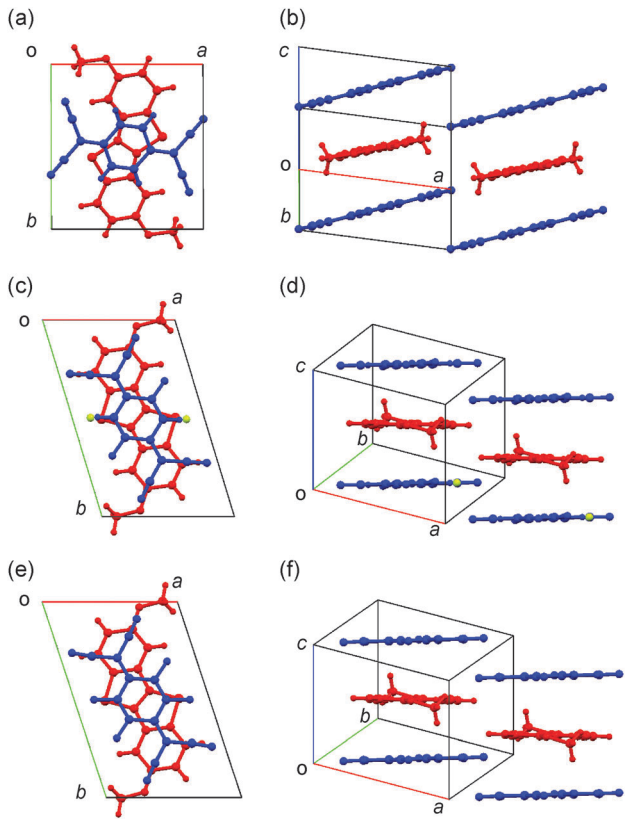

Fig. 2 Crystal structures and transfer integrals of CT complexes: (a and b) (DMeO-BTBT)(TCNQ), (c and d) (DMeO-BTBT)(F_2-TCNQ), and (e and f) (DMeO-BTBT)(F_4-TCNQ). Projection along (a, c and e) the stacking direction and (b, d and f) the molecular long axis of DMeO-BTBT.

In the crystal of (DMeO-BTBT)(TCNQ), the molecular long axis of the donor is approximately perpendicular to the acceptor long axis. In the crystals of (DMeO-BTBT)(F_2-TCNQ) and (DMeO-BTBT)(F_4-TCNQ), however, the long axes of the donor and acceptor molecules are almost parallel. Crystals of (DMeO-BTBT)(F_2-TCNQ) and (DMeO-BTBT)(F_4-TCNQ) are isostructural as evident from the lattice constants (Table 1). The *ac* lattice is approximately the same as the *ab* lattice of the alkyl BTBT complexes (7.8 Å × 7.1 Å),[11a] to indicate the structure of the core stacks are identical. In contrast, (DMeO-BTBT)(TCNQ) has an obviously different lattice.

All crystals have C–H···N hydrogen bonds between the C_{sp^2}–H part of DMeO-BTBT and the C≡N group of TCNQ derivatives. In (DMeO-BTBT)(TCNQ), the C–H···N distance of 2.579 Å, which is shorter than the sum of the van der Waals radii of these atoms (2.75 Å), is observed through the 4-position C_{sp^2}–H of DMeO-BTBT, leading to the orthogonal BTBT-TCNQ alignment (Fig. S4, ESI†). On the other hand, (DMeO-BTBT)(F_2-TCNQ) and (DMeO-BTBT)(F_4-TCNQ) has the short C–H···N distances (2.649 and 2.669 Å, respectively) through the 2-position C_{sp^2}–H of BTBT moiety bringing about the parallel arrangement. Furthermore, in (DMeO-BTBT)(TCNQ), a methoxy oxygen of DMeO-BTBT has a C–H···O interaction with the TCNQ hydrogen atom in the adjacent column (Fig. S5, ESI†). The H···O distance is 2.757 Å, implying the formation of the network of the very weak hydrogen bonding.[26] By contrast, (DMeO-BTBT)(F_2-TCNQ) and (DMeO-BTBT)(F_4-TCNQ) do not have such a hydrogen bond. Therefore, the hydrogen bonding is associated with the orthogonal donor–acceptor alignment.

The charge-transfer degrees estimated from the bond lengths of the TCNQ molecules (ESI†) are small, so the present TCNQ complexes are essentially regarded as neutral complexes.

The effective transfer integrals for holes and electrons (t_h^{eff} and t_e^{eff}) are estimated by an energy-splitting approach for the D–A–D (t_h^{eff}) and A–D–A (t_e^{eff}) triads (Table 2 and Fig. S6–S8, ESI†).[27] The resulting values are 20–70 meV. In the TCNQ complex, t_h^{eff} and t_e^{eff} are comparable, whereas in the F_2-TCNQ and F_4-TCNQ complexes, t_e^{eff} is predominant. This is attributed to the difference of the parallel and perpendicular molecular arrangements.

Thin-film properties

X-ray diffraction (XRD) patterns, and atomic force microscopy (AFM) images of the thin films deposited on the tetratetracontane

Table 2 Effective transfer integrals

Crystal	t_h^{eff} (meV)	t_e^{eff} (meV)
(DMeO-BTBT)(TCNQ)	37	55
(DMeO-BTBT)(F_2-TCNQ)	23	71
(DMeO-BTBT)(F_4-TCNQ)	21	75

(TTC)-modified Si/SiO_2 substrate were obtained. As shown in Fig. 3a, the XRD patterns show diffraction peaks around $2\theta = 7.9^\circ$ attributed to the CT complexes (d = 11.1–11.4 Å). These d-spacings correspond to the $b \sin\alpha \sin\gamma$ of the crystal lattice in (DMeO-BTBT)(F_2-TCNQ) and (DMeO-BTBT)(F_4-TCNQ), indicating that the crystallographic ac plane is aligned parallel to the substrate. In (DMeO-BTBT)(TCNQ), the observed d-spacing does not coincide with the crystal lattice, but is very close to the d-spacing of the other complexes. This suggests the thin-film phase is different from the crystal phase, and isostructural to the other crystals, where the donor long axis is almost parallel to the acceptor long axis. In the thin film of (DMeO-BTBT)(TCNQ), another small peak is observed at $2\theta \sim 10.3^\circ$ (d = 8.6 Å). This d-spacing correspond to the a-axis of the crystal lattice, indicating the presence of a small amount of the crystal phase. (DMeO-BTBT)(F_2-TCNQ) shows a diffraction peak boarder than the others as indicated by the comparatively large full width at half maximum (FWHM) in Fig. 3a. This is associated with the disordered arrangement of the F_2-TCNQ complex. The small peak of (DMeO-BTBT)(TCNQ) coming from the single-crystal phase ($2\theta = 10.3^\circ$) also shows a large FWHM, which suggests comparatively poor crystallinity of the crystal phase in the thin films. AFM images of the evaporated thin films are shown in Fig. 3b–d. In all thin films, needle-like microcrystals cover the substrate densely. The thin film of (DMeO-BTBT)(TCNQ) shows relatively larger roughness than (DMeO-BTBT)(F_2-TCNQ) and (DMeO-BTBT)(F_4-TCNQ). This may be related to the presence of the two phases. In contrast, the other thin films consisting of one kind of layer structure show comparatively smooth surface.

Transistor properties

Transfer and output characteristics of the single-crystal transistors are shown in Fig. 4. The device parameters are summarized in Table 3. The CT complexes show n-channel transistor properties both in vacuum and in air. It has been generally

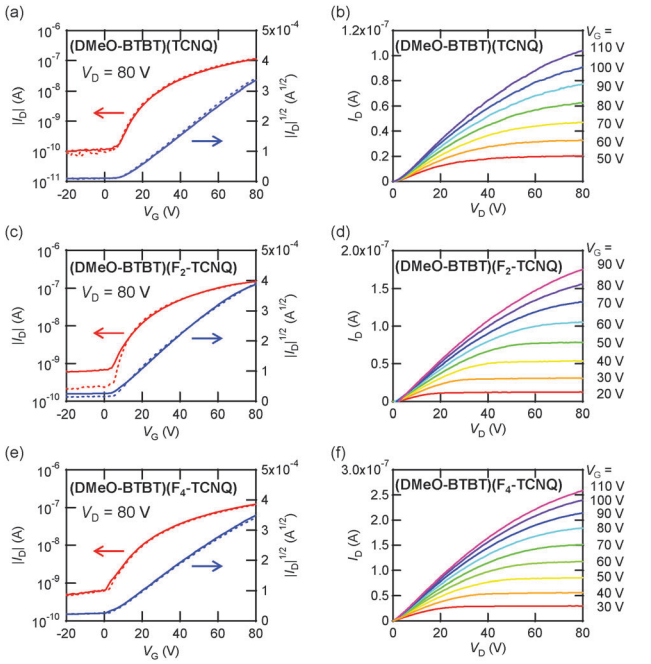

Fig. 4 Typical transfer and output characteristics for single-crystal transistors of (DMeO-BTBT)(F_n-TCNQ) (n = 0, 2, and 4). (a and b): n = 0, (c and d): n = 2, and (e and f): n = 4. The solid transfer characteristics are measured in vacuum and the dotted characteristics in air.

observed that mixed-stack CT complexes containing TCNQ show only n-channel transistor properties, though ambipolar properties are reported in a few single-crystal transistors.[11–14] In addition, we have to mention the comparatively weak donor ability of DMeO-BTBT (Fig. 5), where electron injection to F_n-TCNQ is preferable to hole injection to DMeO-BTBT.[13c] Neutral DMeO-BTBT does not show any transistor properties in the form of either single crystals or thin films. The crystal structure of DMe-BTBT (Fig. 1) is entirely different from the herringbone structure of alkyl-BTBT, and the large molecular displacement and the resulting small intermolecular overlap are responsible for the absence of the transistor properties.

Among the thin-film transistors, the highest electron mobility of 0.022 $cm^2 V^{-1} s^{-1}$ is observed in (DMeO-BTBT)(F_4-TCNQ) in vacuum. The mobility increases in the order of TCNQ < F_2-TCNQ < F_4-TCNQ. This order is potentially related to the

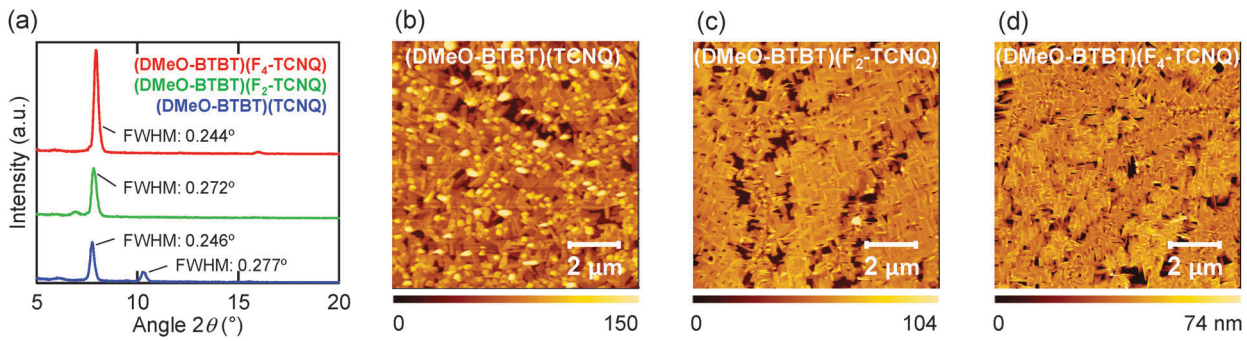

Fig. 3 (a) XRD patterns and AFM images of (b) (DMeO-BTBT)(TCNQ), (c) (DMeO-BTBT)(F_2-TCNQ), and (d) (DMeO-BTBT)(F_4-TCNQ) thin films (50 nm) deposited on 20 nm TTC.

Table 3 Transistor characteristics for thin-film and single-crystal devices of (DMeO-BTBT)(F_n-TCNQ) (n = 0, 2, and 4)

Devices	Acceptors	Conditions	μ_{av} [μ_{max}] ($cm^2\ V^{-1}\ s^{-1}$)	V_{th} (V)	On/off
Thin-film	TCNQ	In vacuum	2.1×10^{-4} [4.7×10^{-4}]	30	10^3
		In air	1.2×10^{-5} [1.8×10^{-5}]	33	10^3
	F_2-TCNQ	In vacuum	6.3×10^{-4} [7.3×10^{-4}]	29	10^3
		In air	6.6×10^{-4} [8.2×10^{-4}]	48	10^3
		In air (after one year)	1.4×10^{-3} [1.6×10^{-3}]	70	10^3
	F_4-TCNQ	In vacuum	6.7×10^{-3} [0.022]	10	10^3
		In air	2.0×10^{-3} [2.5×10^{-3}]	27	10^3
		In air (after one year)	2.6×10^{-3} [2.7×10^{-3}]	7	10^3
Single-crystal	TCNQ	In vacuum	0.016 [0.060]	18	10^3
		In air	0.015 [0.055]	19	10^3
		In air (after one year)	0.047 [0.060]	15	10^3
	F_2-TCNQ	In vacuum	0.033 [0.097]	4	10^2
		In air	0.024 [0.060]	9	10^2
	F_4-TCNQ	In vacuum	0.018 [0.049]	−1	10^2
		In air	0.021 [0.049]	2	10^2

film quality (Fig. 3); the XRD intensity increases, and the AFM roughness decreases in this order. However, since the mobilities of the thin-film devices are to some extent reduced in air, we could not exclude the potential influence of the improved acceptor ability (Fig. 5).

By contrast, the single-crystal transistors do not show a systematic increase, and all complexes exhibit similar mobilities in the order of 10^{-2} $cm^2\ V^{-1}\ s^{-1}$. The highest mobility is 0.097 $cm^2\ V^{-1}\ s^{-1}$ in (DMeO-BTBT)(F_2-TCNQ), but other complexes show mobilities of the same order. This value is not largely different from 0.4 $cm^2\ V^{-1}\ s^{-1}$ reported in (C*n*BTBT)(TCNQ)-based single-crystal transistors.[11] The transistor properties of the single-crystal transistors do not change in air. This is obvious from Fig. 4 as well as the mobility values in Table 3. The performance in air is practically unchanged even after one-year storage (Table 3 and Fig. S10, ESI†); note that the mobility values listed in Table 3 even slightly increase after one-year storage. It should be also pointed out that the threshold voltage V_{th} is large in the thin-film transistors (Table 3), and increases in air. In contrast, V_{th} is small in the single-crystal transistors, particularly in the F_4-TCNQ complex. In general, it is difficult to realize air-stable n-channel organic transistors because the presence of gaseous water and oxygen reduces the performance.[31]

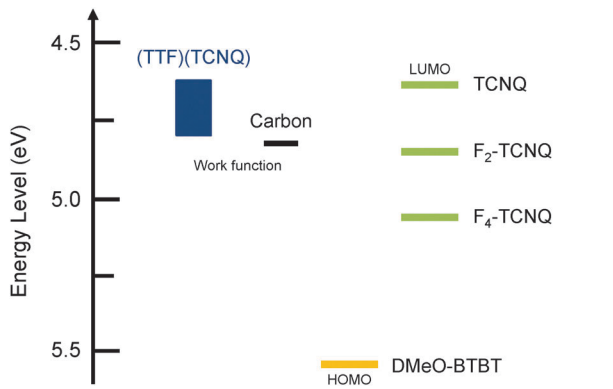

Fig. 5 HOMO level of DMeO-BTBT, LUMO levels of TCNQ derivatives,[28] and the Fermi levels of (TTF)(TCNQ),[29] and carbon.[30]

This particularly applies to thin-film transistors, and among the present combinations, even F_4-TCNQ is insufficient to entirely eliminate the drop of the mobility and the shift of V_{th} in air. The present work demonstrates that the single-crystal transistors are almost free from such instabilities. This is probably because water and oxygen do not penetrate into the crystals. As a result, TCNQ is sufficient to achieve the air-stable performance.

Conclusions

We have prepared a new donor molecule DMeO-BTBT and investigated the crystal structure and transistor properties of the CT complexes (DMeO-BTBT)(F_n-TCNQ) (n = 0, 2, and 4). The thin-film and single-crystal transistors show n-channel transistor properties even in air. Although the performance and stability of the thin-film transistors are considerably influenced by the acceptor strength, the single-crystal transistors are particularly stable in air, and even the TCNQ complex is sufficient to achieve the excellent air stability. Since it is still difficult to realize air-stable n-channel organic transistors, the use of the CT complexes is an important strategy, where these TCNQ complexes achieve fairly good performance in spite of the mixed stack structures. The present work demonstrates, in such a case, the single-crystal transistors show remarkably improved stability in comparison with the thin-film transistors.

Acknowledgements

The authors are grateful to Center for Advanced Materials Analysis, Tokyo Institute of Technology, for X-ray diffraction measurements. The authors also gratefully acknowledge Prof. H. Mori, The University of Tokyo, for the DFT calculation using the Gaussian 03 package.

Notes and references

1 C. D. Dimitrakopoulos and P. R. L. Malenfant, *Adv. Mater.*, 2002, **14**, 99.
2 C. Wang, H. Dong, W. Hu, Y. Liu and D. Zhu, *Chem. Rev.*, 2012, **112**, 2208.

3 A. R. Murphy and J. M. J. Frechet, *Chem. Rev.*, 2007, **107**, 1066.
4 V. Coropceanu, J. Cornil, D. A. S. Filho, Y. Olivier, R. Silbey and J. L. Brédas, *Chem. Rev.*, 2007, **107**, 926.
5 K. Takimiya, S. Shinamura, I. Osaka and E. Miyazaki, *Adv. Mater.*, 2011, **23**, 12604.
6 (*a*) K. Takimiya, H. Ebata, K. Sakamoto, T. Izawa, T. Otsubo and Y. Kunugi, *J. Am. Chem. Soc.*, 2006, **128**, 12604; (*b*) A. Y. Amin, A. Khassanov, K. Reuter, T. Meyer-Friedrichsen and M. Halik, *J. Am. Chem. Soc.*, 2012, **134**, 16548; (*c*) H. Iino, T. Usui and J. Hanna, *Nat. Commun.*, 2015, **6**, 6828.
7 (*a*) H. Ebata, T. Izawa, E. Miyazaki, K. Takimiya, M. Ikeda, H. Kuwabara and T. Yui, *J. Am. Chem. Soc.*, 2007, **129**, 15732; (*b*) T. Izawa, E. Miyazaki and K. Takimiya, *Adv. Mater.*, 2008, **20**, 3388; (*c*) A. Kumatani, C. Liu, Y. Li, P. Darmawan, K. Takimiya, T. Minari and K. Tsukagoshi, *Sci. Rep.*, 2012, **2**, 393; (*d*) Y. Li, C. Liu, Y. Wang, Y. Yang, X. Wang, Y. Shi and K. Tsukagoshi, *AIP Adv.*, 2013, **3**, 052123; (*e*) H. Minemawari, J. Tsutsumi, S. Inoue, T. Yamada, R. Kumai and T. Hasegawa, *Appl. Phys. Express*, 2014, **7**, 091601; (*f*) G. Schweicher, V. Lemaur, C. Niebel, C. Ruzié, Y. Diao, O. Goto, W.-Y. Lee, Y. Kim, J.-B. Arlin, J. Karpinska, A. R. Kennedy, S. R. Parkin, Y. Olivier, S. C. B. Mannsfeld, J. Cornil, Y. H. Geerts and Z. Bao, *Adv. Mater.*, 2015, **27**, 3066.
8 (*a*) T. Uemura, Y. Hirose, M. Uno, K. Takimiya and J. Takeya, *Appl. Phys. Express*, 2009, **2**, 111501; (*b*) H. Minemawari, T. Yamada, H. Matsui, J. Tsutsumi, S. Haas, R. Chiba, R. Kumai and T. Hasegawa, *Nature*, 2011, **475**, 364; (*c*) Y. Yuan, G. Giri, A. L. Ayzner, A. P. Zoombelt, S. C. B. Mannsfeld, J. Chen, D. Nordlund, M. F. Toney, J. Huang and Z. Bao, *Nat. Commun.*, 2014, **5**, 3005.
9 H. Méndez, G. Heimel, A. Opitz, K. Sauer, P. Barkowski, M. Oehzelt, J. Soeda, T. Okamoto, J. Takeya, J. B. Arlin, J. Y. Balandier, Y. Geerts, N. Koch and I. Salzmann, *Angew. Chem., Int. Ed.*, 2013, **52**, 7751.
10 (*a*) T. Kadoya, M. Ashizawa, T. Higashino, T. Kawamoto, S. Kumeta, H. Matsumoto and T. Mori, *Phys. Chem. Chem. Phys.*, 2013, **15**, 17818; (*b*) Y. Kiyota, T. Kadoya, K. Yamamoto, K. Iijima, T. Higashino, T. Kawamoto, K. Takimiya and T. Mori, *J. Am. Chem. Soc.*, 2016, **138**, 3920; (*c*) T. Higashino, T. Kadoya, S. Kumeta, K. Kurata, T. Kawamoto and T. Mori, *Eur. J. Inorg. Chem.*, 2014, 3895.
11 (*a*) J. Tsutsumi, S. Matsuoka, S. Inoue, H. Minemawari, T. Yamada and T. Hasegawa, *J. Mater. Chem. C*, 2015, **3**, 1976; (*b*) Y. Shibata, J. Tsutsumi, S. Matsuoka, K. Matsubara, Y. Yoshida, M. Chikamatsu and T. Hasegawa, *Appl. Phys. Lett.*, 2015, **106**, 143303.
12 (*a*) J. Zhang, H. Geng, T. S. Virk, Y. Zhao, J. Tan, C. Di, W. Xu, K. Shingh, W. Hu, Z. Shuai, Y. Liu and D. Zhu, *Adv. Mater.*, 2012, **24**, 2603; (*b*) D. Vermeulen, L. Y. Zhu, K. P. Goetz, P. Hu, H. Jiang, C. S. Day, O. D. Jurchescu, V. Coropceanu, C. Kloc and L. E. McNeil, *J. Phys. Chem. C*, 2014, **118**, 24688; (*c*) W. Zhu, Y. Yi, Y. Zhen and W. Hu, *Small*, 2015, **11**, 2150.
13 (*a*) T. Hasegawa, K. Mattenberger, J. Takeya and B. Batlog, *Phys. Rev. B: Condens. Matter Mater. Phys.*, 2004, **69**, 245115; (*b*) Y. Takahashi, T. Hasegawa, Y. Abe, Y. Tokura, K. Nishimura and G. Saito, *Appl. Phys. Lett.*, 2005, **86**, 063504; (*c*) Y. Takahashi, T. Hasegawa, Y. Abe, Y. Tokura and G. Saito, *Appl. Phys. Lett.*, 2006, **88**, 073504.
14 (*a*) K. Shibata, K. Ishikawa, H. Takezoe, H. Wada and T. Mori, *Appl. Phys. Lett.*, 2008, **92**, 023305; (*b*) J. Inoue, M. Kanno, M. Ashizawa, C. Seo, A. Tanioka and T. Mori, *Chem. Lett.*, 2010, **39**, 538.
15 T. Takahashi, S. Tamura, Y. Akiyama, T. Kadoya, T. Kawamoto and T. Mori, *Appl. Phys. Express*, 2012, **5**, 061601.
16 (*a*) E. Menard, V. Podzorov, S. H. Hur, A. Gaur, M. E. Gershenson and J. A. Rogers, *Adv. Mater.*, 2004, **16**, 2097; (*b*) M. Yamagishi, Y. Tominari, T. Uemura and J. Takeya, *Appl. Phys. Lett.*, 2009, **94**, 053305; (*c*) Y. Krupskaya, M. Gibertini, N. Marzari and A. F. Morpurgo, *Adv. Mater.*, 2015, **27**, 2453.
17 (*a*) Y. Yamashita, *Chem. Lett.*, 2009, **38**, 870; (*b*) Y. Wen and Y. Liu, *Adv. Mater.*, 2010, **22**, 1331; (*c*) X. Gao, C. Di, Y. Hu, X. Yang, H. Fan, F. Zhang, Y. Liu, H. Li and D. Zhu, *J. Am. Chem. Soc.*, 2010, **132**, 3697; (*d*) H. Usta, A. Facchetti and T. J. Marks, *Acc. Chem. Res.*, 2011, **44**, 501; (*e*) X. Zhan, A. Facchetti, S. Barlow, T. J. Marks, M. A. Ratner, M. R. Wasielewki and S. R. Marder, *Adv. Mater.*, 2011, **23**, 268; (*f*) Y. Hu, X. Gao, C. Di, X. Yang, F. Zhang, Y. Liu, H. Li and D. Zhu, *Chem. Mater.*, 2011, **23**, 1204; (*g*) L. Tan, Y. Guo, G. Zhang, Y. Yang, D. Zhang, G. Yu, W. Xu and Y. Liu, *J. Mater. Chem.*, 2011, **21**, 18042; (*h*) Y. Qiao, Y. Guo, C. Yu, F. Zhang, W. Xu, Y. Liu and D. Zhu, *J. Am. Chem. Soc.*, 2012, **134**, 4084; (*i*) F. Zhang, Y. Hu, T. Schuettfort, C. Di, X. Gao, C. R. McNeill, L. Thomsen, S. C. B. Mannsfeld, W. Yuan, H. Sirringhaus and D. Zhu, *J. Am. Chem. Soc.*, 2013, **135**, 2338; (*j*) X. Gao and Y. Hu, *J. Mater. Chem. C*, 2014, **2**, 3099; (*k*) A. Filatre-Furcate, T. Higashino, D. Lorcy and T. Mori, *J. Mater. Chem. C*, 2015, **3**, 3569.
18 B. L. Flynn, P. Verdier-Pinard and E. Hamel, *Org. Lett.*, 2001, **5**, 651.
19 M. J. Mio, L. C. Kopel, J. B. Braun, T. L. Gadzikwa, K. L. Hull, R. G. Brisbois, C. J. Markworth and P. A. Grieco, *Org. Lett.*, 2002, **19**, 3199.
20 (*a*) M. Kraus, S. Richler, A. Opitz, W. Brütting, S. Haas, T. Hasegawa, A. Hinderhofer and F. Schreiber, *J. Appl. Phys.*, 2010, **107**, 094503; (*b*) M. Kraus, S. Haug, W. Brütting and A. Opitz, *Org. Electron.*, 2011, **12**, 731.
21 L. B. Coleman, M. J. Cohen, D. J. Sandman, F. G. Yamagishi, A. F. Gartio and A. J. Heeger, *Solid State Commun.*, 1973, **12**, 1125.
22 (*a*) K. Shibata, H. Wada, K. Ishikawa, H. Takezoe and T. Mori, *Appl. Phys. Lett.*, 2007, **90**, 193509; (*b*) T. Kadoya, D. de Caro, K. Jacob, C. Faulmann, L. Valade and T. Mori, *J. Mater. Chem.*, 2011, **21**, 18421.
23 (*a*) S. Tamura, T. Kadoya, T. Kawamoto and T. Mori, *Appl. Phys. Lett.*, 2013, **102**, 063305; (*b*) S. Tamura, T. Kadoya and T. Mori, *Appl. Phys. Lett.*, 2014, **105**, 023301.
24 J. Cho, T. Higashino and T. Mori, *Appl. Phys. Lett.*, 2015, **106**, 193303.

25 A. Aumuller, P. Erk, S. Hunig, E. Hadicke, K. Peters and H. G. von Schnering, *Chem. Ber.*, 1991, **124**, 2001.
26 (*a*) J. R. Desiraju, *Acc. Chem. Res.*, 1991, **24**, 290; (*b*) T. Higashino, S. Kumeta, S. Tamura, Y. Ando, K. Ohmori, K. Suzuki and T. Mori, *J. Mater. Chem. C*, 2015, **3**, 1588.
27 (*a*) L. Zhu, Y. Yi, Y. Li, E.-G. Kim, V. Coropceanu and J.-L. Brédas, *J. Am. Chem. Soc.*, 2012, **134**, 2340; (*b*) L. Zhu, Y. Yi, A. Fonari, N. S. Corbin, V. Coropceanu and J.-L. Brédas, *J. Phys. Chem. C*, 2014, **118**, 14150; (*c*) H. Geng, X. Zheng, Z. Shuai, L. Zhu and Y. Yi, *Adv. Mater.*, 2015, **27**, 1443.
28 S.-S. Pac and G. Saito, *J. Solid State Chem.*, 2002, **168**, 486.
29 (*a*) C. R. Newman, C. D. Frisbie, D. A. da Silva Filho, J.-L. Bredas, P. C. Ewbank and K. R. Mann, *Chem. Mater.*, 2004, **16**, 4436; (*b*) T. Mori, *Chem. Lett.*, 2011, **40**, 428; (*c*) D. de Caro, K. Jacob, H. Hahioui, C. Faulmann, L. Valade, T. Kadoya, T. Mori, J. Fraxedas and L. Viau, *New J. Chem.*, 2011, **35**, 1315.
30 M. Shiraishi and M. Ata, *Carbon*, 2001, **39**, 1913.
31 (*a*) D. M. de Leeuw, M. M. J. Simenon, A. R. Brown and R. E. F. Einerhand, *Synth. Met.*, 1997, **87**, 53; (*b*) D. Shukla, S. F. Nelson, D. C. Freeman, M. Rajeswaran, W. G. Ahearn, D. M. Meyer and J. T. Carey, *Chem. Mater.*, 2008, **20**, 7486; (*c*) Y. Ie, M. Ueta, M. Nitani, N. Tohnai, M. Miyata, H. Tada and Y. Aso, *Chem. Mater.*, 2012, **24**, 3285.